HHS Public Access

Author manuscript

Nat Struct Mol Biol. Author manuscript; available in PMC 2013 September 01.

Published in final edited form as:

Nat Struct Mol Biol. 2013 March ; 20(3): 363–370. doi:10.1038/nsmb.2500.

A recurring motif for antibody recognition of the receptor-binding site of influenza hemagglutinin

Rui Xu[1], **Jens C. Krause**[2], **Ryan McBride**[4], **James C. Paulson**[1,4], **James E. Crowe Jr.**[2,3,†], and **Ian A. Wilson**[1,5,†]

[1]Department of Molecular Biology, The Scripps Research Institute, La Jolla, California, USA

[2]Department of Pediatrics, Vanderbilt University Medical Center, Nashville, Tennessee, USA

[3]Department of Pathology, Microbiology and Immunology, Vanderbilt University Medical Center, Nashville, Tennessee, USA

[4]Department of Chemical Physiology, The Scripps Research Institute, La Jolla, California, USA

[5]Skaggs Institute for Chemical Biology, The Scripps Research Institute, La Jolla, California, USA

Abstract

Influenza virus hemagglutinin (HA) mediates receptor binding and viral entry during influenza infection. The development of receptor analogs as viral entry blockers has not been successful, suggesting that sialic acid may not be an ideal scaffold to obtain broad and potent HA inhibitors. Here we report crystal structures of Fab fragments from three human antibodies that neutralize the 1957 pandemic H2N2 influenza virus in complex with H2 HA. All three antibodies use an aromatic residue to plug a conserved cavity in the HA receptor-binding site. Each antibody interacts with the absolutely conserved HA1 Trp153 at the cavity base through π-π stacking with the signature Phe54 of two V_H1-69 antibodies or a tyrosine from HCDR3 in the other antibody. This remarkably conserved interaction can be used as a starting point to design inhibitors targeting this conserved hydrophobic pocket in influenza viruses.

Influenza viruses cause substantial morbidity and mortality through seasonal epidemics and occasional pandemics. Vaccination has been an effective approach in prevention of influenza infections against seasonal influenza, but not against pandemic viruses. The constant antigenic drift of circulating viruses, as well as the vast diversity of zoonotic

†To whom correspondence should be addressed. wilson@scripps.edu; james.crowe@vanderbilt.edu.

Accession codes. Protein Data Bank: coordinates and structure factors have been deposited with accession codes 4HF5, 4HFU and 4HG4.

Note: Supplementary information is available in the online version of the paper.

Competing financial interests

Vanderbilt University previously submitted a patent covering the diagnostic and therapeutic use of antibodies 2G1, 8M2 and 8F8 prior to the structural work described here.

Author contributions

R.X., J.C.K., J.E.C and I.A.W. designed the research; R.X., J.C.K. and R.M. performed the research; R.X., J.C.K., R.M., J.C.P., J.E.C and I.A.W. analyzed data; J.E.C and I.A.W. supervised the project; and R.X., J.C.K., J.E.C., and I.A.W. wrote the manuscript.

viruses that might enter the human population, pose persistent threats to human health. In the event of a pandemic outbreak, vaccine production against the emerging virus would lag several months behind the emergence of the new virus. Thus, prevention or treatment strategies that can cover a broad range of viral strains and subtypes are urgently needed. Currently, antiviral strategies in development include universal influenza vaccines [1], broadly neutralizing therapeutic antibodies [2] and small molecule inhibitors [3].

The hemagglutinin (HA) is the major surface envelope protein of influenza A and B viruses. It carries essential functions in the viral life cycle. Viral entry is mediated by attachment through HA binding to sialic acid receptors on the host membrane and then internalization of viral particles into the late endosome [4]. The HA receptor-binding site is a shallow depression in the globular head at the extreme membrane-distal end of HA, and is surrounded by structural elements commonly referred to as the 220 loop, 130 loop, 150 loop and 190 helix, named after their sequence numbers in the mature HA protomer [4]. Although HAs of different subtypes from different hosts display some unique structural features around the receptor-binding pocket, which determine their fine specificity and avidity, a large portion of the receptor-binding site is highly conserved for the recognition of the common ligand, the terminal sialic acid of sialyated glycans. Most notably, a hydrophobic cavity at the 150 loop end of the receptor-binding site, which accommodates the 5-acetamido moiety of sialic acid, is formed by universally conserved HA residues Trp153, Leu194, Tyr195 and other conserved residues from the 130 and 150 loops.

The exposed receptor-binding site pocket has been of interest for inhibitor design since the identification of sialic acid as the viral receptor [5] and the structural determination of HA in complex with sialic acid [6] in the 1980s. However, design of sialic acid analogs as inhibitors has failed to yield high-affinity binders to the shallow receptor-binding site with broad specificity against human-infecting HA subtypes [7], probably because sialic acid itself is a low-affinity binder (low mM) [8]. Derivatives of Neu5Ac often improve their affinity only through acquiring additional interactions with nonconserved HA residues near the receptor-binding site. Recent approaches have used polyvalent presentation of sialic acid analogs to enhance their inhibitory activity by mimicking the multivalent binding between virus and host cell [7]. However, these applications have raised concern of toxicity and drug delivery [7]. Research in the last three decades suggests that Neu5Ac presents an insurmountable challenge for drug design at the receptor-binding pocket and a new chemical scaffold that can access novel ligand-HA interactions is urgently needed.

The receptor-binding site of HA presents also a potential target for engagement with antibodies. Because the receptor-binding site must be exposed for binding to host glycan receptors, this site cannot be blocked by the dense glycan shield that is used by some viruses to mask surveillance by the host immune system [9, 10]. However, most previously known epitopes map to the most accessible hypervariable regions, which surround the receptor-binding site, and are not well conserved among different influenza subtypes and strains [11]. Antibodies to these hypervariable loops select for escape mutants, which, on a population level, lead to antigenic drift. In recent months, antibody identification efforts, coupled in some cases with structural studies, have revealed that the receptor-binding site of HA itself also can serve as a main site for antibody-antigen interactions. Human antibodies CH65 and

C05, and murine antibody S139/1, each insert a complementarity determining region (CDR) loop into the receptor-binding site [12–14]. Several antibodies encoded by the human V_H1-69 gene segment also were proposed to recognize epitopes at or near the receptor-binding pocket of HA [15,16]. Unlike most HA head antibodies, these receptor-binding site antibodies showed a surprising ability to broadly neutralize a large number of strains from a single HA subtype or selected strains from different subtypes and groups of influenza viruses. CH65 neutralizes a wide spectrum of seasonal H1 viruses isolated in the past 30 years [12]. S139/1 was the first head-specific antibody to be described to neutralize strains from different subtypes (H1, H2, H3, and H13) and from the two phylogenetic lineages (group 1 and 2) of influenza A viruses [17]. C05 has similar breadth and binds and/or neutralizes selected strains from H1, H2, H3, H9 and H12 subtypes [13]. Human V_H1-69-encoded antibody F045-092 also has been reported to cross-neutralize strains from multiple subtypes (H1, H2, H3, H5) [15]. Thus, these antibodies do not simply block the receptor-binding site, but must have a footprint that avoids interaction with many of the hypervariable residues surrounding the receptor-binding site, at least within subtypes or across selected strains from different subtypes.

We recently described the first naturally occurring human monoclonal antibodies (mAbs) specific for the globular head of H2N2 influenza HA, mAbs 8F8, 8M2, and 2G1, that were generated with hybridoma technology from the peripheral blood of middle-aged donors [16]. These three antibodies showed a similar spectrum, reacting with human H2N2 viruses that circulated between 1957 to 1963, as well as a swine H2N3 strain isolated in 2006 [16]. Antibody 2G1 also showed hemagglutination inhibition (HAI) activity against a tested H3 strain (A/Hong Kong/1/1968) [16]. H2N2 was the sole influenza A virus in human circulation between 1957 and 1968, causing several epidemics [18,19] and an excess mortality of up to 66,000 deaths in the 1957–58 pandemic season in the US alone [20]. It is estimated that up to four million people worldwide died due to influenza A over this 12-year period [21]. H2N2 has not recurred in humans, but strains similar to the 1957 pandemic strain continue to circulate in avian [22–24] and swine [23] reservoirs. As human herd immunity to H2N2 wanes, these H2 viruses have increasing potential to reenter the human population from these animal reservoirs [21].

Here, we set out to study the structural basis of neutralization by these human H2 antibodies. The fragment antigen-binding regions (Fabs) of the three H2 neutralizing antibodies were crystallized and their structures determined in complex with H2 HA to elucidate their mode of binding and mechanism of neutralization. These three antibodies, in conjunction with the reports of other head-binding antibodies [12,13], have uncovered novel mechanisms of neutralization and provide chemical scaffolds that may aid in the design of drugs against the receptor-binding site pocket.

Results

Antibodies 2G1 and 8M2

Germline V_H1-69 is the only human heavy-chain gene segment that encodes two hydrophobic residues at the tip of CDR2 loop: namely Ile53 and Phe54 (ref 25). Antibodies derived from this germline gene segment are known to bind to conserved hydrophobic

pockets on the envelope proteins of hepatitis C virus (HCV) [26–28], human immunodeficiency virus (HIV) [25,29,30] and the stem region of influenza A viruses [31,32]. Germline gene V_H1-69-encoded stem-region antibodies of flu HA target a conserved hydrophobic patch on the HA stem that is not fully protected by glycosylation. In the last few months, some V_H1-69-encoded antibodies have been described that appear to recognize epitopes near the HA receptor-binding site, but the exact structural nature of such antibody recognitions has not been elucidated [15,16]. Here, we determined the crystal structures of H2 HA (A/Japan/305+/1957) in complex with the Fab fragments of two V_H1-69-encoded antibodies, 2G1 and 8M2, to provide the first structural illustration of how V_H1-69 antibodies bind to the HA receptor-binding site.

Fab fragments of 2G1 and 8M2 were expressed in mammalian cell line 293F suspension culture. Purified Fab and the recombinant H2 HA ectodomain were mixed and passed through a gel filtration column to isolate stable HA–Fab complexes for crystallization. Crystal structures of 8M2–H2 HA and 2G1–H2 HA complexes were determined at 3.1 and 3.2 Å resolution, respectively (Table 1).

Antibodies 2G1 and 8M2 approach the HA receptor-binding site from a similar direction, but completely opposite orientation (Figs. 1A–B). Three Fabs bind per trimer. The heavy chain CDR (HCDR) loops of both antibodies are centered on the HA receptor-binding site, engaging residues in and around the region where sialic acid binds (Fig. 2). The 2G1 light-chain contacts HA residues near the 150 loop that would correspond to the Sa antigenic site in H1 HA (Fig. 2A). In contrast, the 8M2 light-chain contacts the HA around the N-terminal end of the 190 helix, with these interactions being mediated only by light chain CDR 3 (LCDR3) (Figs. 2B, 2D). The heavy chain of both antibodies mediates the majority of the antigen-antibody contacts, contributing to 73% of the buried interface on 2G1 (593 out of 818 $Å^2$) and 84% of the interface on 8M2 (845 out of 1007 $Å^2$) (Figs. 2C–D), as calculated using the Protein Interfaces, Surfaces and Assemblies service (PISA) at European Bioinformatics Institute (http://www.ebi.ac.uk/pdbe/prot_int/pistart.html) [33].

A common feature of 2G1 and 8M2 heavy-chain binding is the insertion of Phe54, one of the signature motifs on HCDR2 of V_H1-69-encoded germline antibodies (Supplementary Fig. 1), into a hydrophobic pocket in the receptor-binding site. In both structures, the aromatic side chain of Phe54 enters a cavity in the receptor-binding site and is buried by conserved hydrophobic residues on the HA (Figs. 3A–B). The phenylalanine aromatic rings are nearly perpendicular to the indole side chain of HA Trp153, and make optimal π-π interactions. Ile53, the other hallmark hydrophobic residue from the V_H1-69 germline sequence at the tip of HCDR2, is also present in both 2G1 and 8M2. Due to differences in the relative antibody orientations, Ile53 contacts different hydrophobic patches in the HA receptor-binding site in the two structures. Ile53 interacts with the 190 helix in the 2G1 complex, whereas it forms van der Waals contacts with the 130 loop in the 8M2 complex (Figs. 3A–B). Furthermore, this Ile53 and Phe54 hydrophobic pair provides 199$Å^2$ and 207 $Å^2$ to the HA-antibody interface in 2G1 and 8M2, respectively.

The antibody–antigen interactions are otherwise different in the 8M2 and 2G1 complexes due to the difference in antibody orientation. The heavy-chain of 8M2 sits atop the receptor-

binding site and completely blocks the entry of glycan receptors. HCDR2 and HCDR3 extend into the receptor-binding site and make extensive contacts to HA residues lining this site (Fig. 3B). The HCDR2 loop is positioned on the 150-loop side of the receptor-binding site. Aside from the hydrophobic contacts mediated by Ile53 and Phe54, the Ser56-Pro57-Asn58 segment of HCDR2 interacts with the HA 150 loop via van der Waals contacts and hydrogen bonds, with the Ser56 hydroxyl hydrogen bonding to Gly158 and Ser159 main-chain nitrogens. Ser56 and Pro57 arose from somatic mutations (Supplementary Fig. 1) and were likely acquired during affinity maturation of antibody 8M2. The HDCR3 loop, on the other hand, reaches into the receptor-binding site pocket from the 220 loop side (Fig. 3B). Glu98 of 8M2 hydrogen bonds with the main-chain nitrogen of HA1 Arg137. The carbonyl oxygen of Gly100 hydrogen bonds with the backbone amides of Gly227 and Ser228. The Trp99 indole of 8M2 lies atop the 190 helix of HA. The tip of HCDR3 main-chain (Gly100 and Ser100A) (antibody residues are listed in the Kabat numbering scheme, with insertions numbered with letters) makes extensive contact with the Leu226 side chain. As a result, 8M2 does not recognize avian-like H2 HAs on blue native polyacrylamide gel electrophoresis (BN-PAGE), which have Gln226 instead of the human-receptor specific Leu226 (data not shown). 8M2 also does not have HAI or neutralization activity against avian-like H2 viruses [16].

In the 2G1 complex, a ridge on the HA surface formed by part of the 150 loop (residues 157–159) serves as the boundary between the binding footprints of the 2G1 heavy and light chains (Fig. 2A). The heavy chain targets the receptor-binding site, and the light chain recognizes part of the β-sheet that roughly corresponds to the Sa antigenic site in the H1 subtype. HCDR2 and HCDR3 insert into the binding site pocket, while HCDR1 touches the 190 helix on the rim of the binding site. Antibody 2G1 HCDR loops only cover about half of the HA receptor-binding site (Fig. 3A). The HCDR2 loop extends toward the conserved HA1 Trp153 from about the middle section of the receptor-binding site. Ile53 and Phe54 at the tip of the HCDR2 are buried inside the receptor-binding pocket. The HCDR2 loop twists at Gly55 and brings Gly55 and Thr56 to close approximation with the 130 loop. These HCDR2 residues are conserved from the germline sequence (Supplementary Fig. 1) and contribute to HA binding. HCDR3 also inserts into the binding pocket, but not as deeply as HCDR2, and covers the upper half of the 150 loop (residues 156–159). Overall, the heavy chain of 2G1 uses 593 $Å^2$ of antibody surface area to bury 543 $Å^2$ of HA at the antibody-HA interface. The interactions mediated by the heavy chain are mostly van der Waals contacts with few polar interactions. The only hydrogen bond is between 2G1 Ser99 and HA1 Thr131 side chains. By comparison, 225 $Å^2$ of the 2G1 light chain surface covers 235 $Å^2$ of HA at the antibody–HA interface.

Thus, the structural analysis of these two antibodies reveals surprising similarities and diversities, and illustrates a common theme for antibody recognition of the most conserved part of the HA receptor-binding site.

8F8–H2 HA complex

The signature π-π interaction between HCDR2 Phe54 and HA Trp153, as employed by the two V_H1-69 germline antibodies, is surprisingly mirrored by a third H2 human antibody 8F8

encoded by a different germline gene segment (V_H3-33). Using similar methods as for 8M2 and 2G1, we determined the crystal structure of Fab 8F8 in complex with H2 HA (an L226Q, S228G mutant of A/Japan/305+/1957) at 3 Å resolution (Fig. 4A, Table 1). The 8F8 heavy chain is encoded by V_H3-33 and its light chain by V_L1-44 (Fig. 4B). Three 8F8 Fabs bind per HA trimer, and approach the receptor-binding site from a similar direction to 8M2 and 2G1, *i.e.*, vertically from the top with respect to the apex of the head domain. The antibody–antigen interface is dominated by the 8F8 heavy chain (Figs. 5A–B), which accounts for 92% of the buried surface area on the Fab (775 out of 847 Å^2) and 91% of the buried interface on the HA (748 out of 827 Å^2). The antibody binding footprint includes absolutely conserved residues at the bottom of the receptor-binding site pocket (Tyr98 and Trp153) that interact with sialic acid, as well as residues from the surrounding structural elements: the 130 loop (residues 131–145 contact antibody), the 150 loop (155–159), the 190 helix (187–196) and the 220 loop (225–226) (Fig. 5A). An avianized H2 HA, which has the avian-like substitutions L226Q and S228G on the 220 loop for binding α2,3 linked sialylated glycans, was used for the crystallization with 8F8. The substitutions do not appear to impact antibody binding, as 8F8 co-migrates with wild type as well as the avianized H2 HA on BN-PAGE (data not shown). The 220 loop contributes only modest surface area (26 Å^2) to 8F8 recognition.

On the antibody side, the centerpiece for antibody–antigen interactions is the HCDR3 loop that is relatively long at 21 amino acids (Figs. 4B, 5B). HCDR3 loop residues provide nearly 70% of the interface area from the antibody (583 out of 847 Å^2) and form a wide bulge with a short helix that nestles into the receptor-binding site. Near the top of the bulge, the Tyr100 aromatic side chain inserts into the hydrophobic pocket surrounded by HA1 Gly134–Gly135, Trp153, Thr155 and Leu194–Tyr195, forming yet another π-π stacking interaction with the conserved HA Trp153. In addition to these extensive hydrophobic interactions, a hydrogen bond is formed between the Tyr100 hydroxyl and the HA1 Thr155 side chain (Fig. 5C). Around Tyr100, the HCDR3 loop snakes through the HA receptor-binding pocket, making extensive hydrophobic contacts, as well as some hydrophilic interactions, with the 130 loop and 150 loop (Fig. 5C). Most notably, Asp97 forms a salt bridge with HA1 Arg137. Ser100A mediates two main-chain hydrogen bonds with HA1 Gly135. On the 150 loop end, HCDR3 Asp100D and Tyr100G hydrogen bond with HA1 Thr155, Glu156 and Gly158. After traversing the receptor-binding site, HCDR3 turns around and adopts a helical structure that makes extensive contacts with the 190 helix that are mostly hydrophobic. On the antibody side, the helix-helix contacts are dominated by three aromatic residues, Tyr100G, His100J and Tyr100K, which together provide 190 Å^2 buried interface on 8F8 (Fig. 5C).

Previously, antibody CH65 was shown to have its HCDR3 inserted into the receptor-binding site of H1 HA [12]. Some similarities are apparent between CH65 and 8F8 binding, with both HCDR3 loops inserting into the elongated HA receptor-binding pocket (Fig. 5D). However, the HCDR3 loops from these two antibodies approach the receptor-binding site from opposite directions and utilize different sets of antibody–antigen interactions. An aspartic acid (Asp100C) on CH65 appears to mimic the sialic acid carboxylate interactions with HA, but a similar contact is absent in the 8F8 complex. Instead, 8F8 HCDR3 inserts more deeply

into the receptor-binding pocket and makes more extensive contacts with conserved residues inside the pocket. 8F8 Tyr100 replaces CH65 Val100B as the residue inserting into the HA hydrophobic cavity above Trp153. A π-π interaction between the antibody and HA Trp153 is absent in the CH65 complex, but is replaced by a hydrophobic interaction. Similarly in antibody S139/1, the pocket is occupied by HCDR2 Met56 (ref 14). In antibody C05, a tryptophan residue from HCDR3 occupies the hydrophobic pocket in HA [17].

Escape mutants and receptor binding

The three H2 antibodies recognize epitopes extensively covering the receptor-binding site of HA. Contrary to many other HA antibodies that target the hypervariable loops in the HA head region, HA escape mutations from these H2 antibodies may interfere with receptor binding, an essential viral function of HA, and impair viral fitness. Escape mutants were selected in chicken eggs in the presence of the H2 antibodies [16]. An escape mutation G135D was selected for antibody 8M2 and a K156E mutation for 2G1. For 8F8, a T193K mutation can escape antibody binding. Another 8F8 escape mutation R137Q greatly reduces HAI activity of 8F8 towards H2N2 virus like particles (VLPs) [22]. These escape mutations are located within the binding footprint of their respective antibodies (Fig. 6A). However, these residue locations on the rim of the receptor-binding pocket might also affect receptor binding. Therefore, we introduced these single mutations on the background of A/Japan/305+/1957 H2 HA and studied their glycan binding activities on a glycan microarray (Figs. 6B–C, Supplementary Fig. 2). The wild-type (WT) HA shows strong binding to a broad spectrum of α2,6-linked glycans, as well as glycans with mixed α2,3 and α2,6 linkages (Fig. 6B). Binding specificity for α2,6, but not α2,3-linked sialylated glycans, is a general property shared by HAs of human viruses. The tested mutations drastically changed the receptor-binding activity of HA. Only the R137Q mutant retained some weak binding for one biantennary glycan (glycan #55) (Fig. 6C), which has a terminal NeuAcα2-6Galβ1-4GlcNAcβ1-3Galβ1-4GlcNAcβ1-3Galβ1-4GlcNAc unit on both arms of the carbohydrate. Binding was not detected for other mutants under the same experimental condition (Supplementary Figs. 2), suggesting greatly diminished or abolished binding for sialic acid receptors in the escape mutants.

In the 12-year circulation of H2N2 viruses in the human population, mutations of G135D, R137Q and K156E were found sporadically in human H2 viruses, but viruses with these mutations did not become established [16]. Instead, later strains (1962–1968) accumulated mutations either at the same positions but with only very subtle changes to the amino-acid properties, or at locations further from the receptor-binding site [16].

Discussion

H2N2 viruses circulated in the human population for 12 years after their introduction during the Asian flu pandemic in 1957. The circulation period of H2N2 viruses was relatively short compared to H1N1 and H3N2 viruses, which have lasted for several decades. It was hypothesized that antibody binding to highly conserved epitopes on the H2 HA may have limited its ability to evolve under human immune selection [34]. One such conserved epitope is the stem region of H2 HA as identified by escape mutations [35].

The receptor-binding site of H2 HA is another highly conserved epitope where antigenic drift could potentially interfere with viral fitness. Three H2 antibodies generated from the peripheral blood of healthy donors all target the receptor-binding pocket and likely block entry of glycan receptor. With the limited number of antibodies studied here, it is difficult to speculate what percentage of H2 antibodies in infected or vaccinated individuals targets the receptor-binding site. However, in a study of murine antibodies, half of the H2 HA antibodies were sensitive to residue changes that are associated with the avian to human HA receptor-specificity switch [36], suggesting that many murine antibodies also target the receptor-binding site of H2 HA and engage HA residues critical for receptor binding.

Antibody recognition of the receptor-binding site presents a challenge for the antigenic drift of viruses, a necessary counter-action against human immune surveillance. Mutations that inhibit antibody binding have to strike a delicate balance in order to inhibit or greatly reduce antibody binding without completely abrogating HA receptor-binding. Escape mutants of antibodies 8F8, 8M2 and 2G1 isolated *in vitro* introduce amino-acid changes into the center of the antibody footprints. While these mutations are effective in abolishing antibody binding, they also reduce HA binding activity, and without compensating mutations, are probably detrimental to the survival of the mutant viruses. In field strains, these same mutations were spotted occasionally, but not inherited by later strains, suggesting they are dead-end mutations. If antibodies such as 2G1, 8M2, or 8F8, were present at the population level, they likely would limit the circulation of H2 viruses in the human population.

Influenza antibodies encoded by the V_H1-69 germline gene segment were conventionally thought of as being stem-specific antibodies. Here, we show that their germline characteristics are also ideally suited for recognition of another structurally conserved influenza functional epitope, the HA receptor-binding pocket. 2G1 and 8M2, two V_H1-69-encoded antibodies studied here, were cloned from two different donors, yet use shared conserved elements of the HCDR2 germline sequence and structure for antigen recognition. These shared structural features are further evidence of antibody convergence [37] toward similar modes of interaction with the receptor-binding site.

Structural analysis of the three antibody complexes presented here along with the recently described C05, CH65 and S139/1 antibody complexes reveals the HA receptor-binding site as a conserved epitope and reveals a potentially druggable pocket inside the HA receptor-binding site. A surprising common theme arises from these three crystal structures. Tyr100 from HCDR3 of antibody 8F8, and Phe54 from HCDR2 of antibodies 2G1 and 8M2, insert their aromatic side chains into a hydrophobic cavity at the 150-loop end of the receptor-binding site (Fig. 7A). Furthermore, CH65 inserts a hydrophobic side chain (Val100B) from HCDR3 into the same cavity [16], C05 positions another aromatic side chain from HCDR3 proximal to Trp153 (ref 13) and S139/1 uses another hydrophobic residue, HCDR2 Met56 (ref 14). During glycan receptor binding, this hydrophobic cavity is occupied by the methyl group from the 5-acetamido of sialic acid (Fig. 7B), suggesting structural conservation here is likely essential for virus receptor binding. In the H2 antibody complexes, the aromatic rings are situated for optimal π-π interaction with HA Trp153 and are surrounded by HA residues Gly134–Gly135, Thr155, Leu194 and Tyr195, all of which are highly conserved in influenza A viruses. Thus, only through structure determination of these H2 antibody

complexes could this recurrent theme be noticed. It is therefore plausible that inhibitors, either small proteins or small molecule compounds, can be designed to target this conserved hydrophobic cavity and mimic the antibody interactions. The presentations of these aromatic residues into the HA hydrophobic cavity provide valuable starting points and novel scaffolds for inhibitor designs. Drug design toward the highly conserved cavity, thus, has the potential to inhibit all influenza A and possibly influenza B HA subtypes.

Online Methods

Fab protein expression and purification

Expression plasmids containing the 8F8, 8M2, or 2G1 heavy or light chain cDNA were generated in modified pEE12.4 or pEE6.4 vectors (Lonza) [16]. In order to express full-length recombinant Fab protein, the heavy chain variable regions with their signal sequences were cut with a HindIII/ApaI double digestion (Fermentas) and ligated with T4 DNA Ligase (New England Biolabs) into the opened 2D1 Fab plasmid [39] with a stop codon immediately after the cysteine of the hinge-disulfide. Plasmid DNA was prepared using a PureYield Plasmid Maxiprep system (Promega) and transfected into 293F suspension culture (Invitrogen) in shaker flasks using PolyFect reagent (Qiagen). After one week, supernatant was purified over a gravity column with CaptureSelect λ resin for 8F8 (BAC B.V., The Netherlands) or with an ÄKTA fast protein liquid chromatography instrument and KappaSelect columns (GE Healthcare) for 8M2, 2G1 and eluted with citrate buffer. The antibodies were buffer-exchanged into PBS via Amicon columns (Millipore) in a swinging-bucket rotor centrifuge. All Fabs expressed in milligram amounts per liter of cell culture supernatant. Purity of the Fab preparations was assessed via reducing, denaturing SDS-PAGE gels.

H2 HA expression and purification

H2 HA ectodomain was expressed using a baculovirus expression system as described previously [34]. Expressed HA was purified through a His-tag affinity purification step and then treated with TPCK (L-1-tosylamide-2-phenylmethyl chloromethyl ketone)-treated trypsin (New England Biolabs). After trypsin digestion, protein sample was purified by gel filtration and concentrated to 1–2 mg/ml in buffer 20 mM Tris, pH8, and 50mM NaCl.

Crystallization and structural determination of the 8F8–H2 complex

An excess of purified, recombinant 8F8 Fab was mixed with H2 HA (L226Q, S228G mutant of A/Japan/305+/1957) and incubated overnight at room temperature to allow complex formation. The optimal ratio was pre-determined by titration of Fab to HA as assayed by gel-shift using Blue Native Polyacrylamide Gel Electrophoresis (BN-PAGE) (Invitrogen). The complex was purified from excess Fab by gel filtration in 20 mM Tris pH 8.0, 50 mM NaCl, and concentrated to 6.2 mg/mL for crystallization. 8F8-H2 complex crystals were grown at 22.5°C in sitting drops by vapor diffusion against a reservoir containing 11% PEG4000, 0.1 M Tris, pH 8.5 and 0.1 M $MgCl_2$. The crystals were cryoprotected by stepwise addition (5% each) of ethylene glycol, up to a final concentration of 25%, and then flash cooled in liquid nitrogen. Diffraction data were collected at 100K on the General Medicine and Cancer Institutes Collaborative Access Team (GM/CA-CAT) 23ID-B

beamline (wavelength: 1.0332 Å) at the Advanced Photon Source at the Argonne National Laboratory and processed with HKL2000 [40]. Initial phases were determined by molecular replacement using Phaser [41]. Refinement was carried out in Phenix [42], alternating with manual rebuilding and adjustment in COOT [43]. Final refinement statistics are summarized in Table 1. In the final model, 92.3% of the residues were in favored regions of the Ramachandran plot, with 7.3% in additional allowed regions.

Crystallization and structural determination of the 2G1–H2 complex

An excess of purified, recombinant 2G1 Fab was mixed with H2 HA (A/Japan/305+/1957) and incubated overnight at 4°C to allow complex formation. The optimal ratio was pre-determined by titration of Fab to HA as assayed by gel-shift using BN-PAGE. The complex was purified from excess Fab by gel filtration in 20 mM Tris pH 8.0, 50 mM NaCl, and concentrated to 12.7 mg/mL for crystallization. 2G1-H2 complex crystals were grown at 22.5°C in sitting drops by vapor diffusion against a reservoir containing 10% PEG6000, 0.1 M HEPES, pH 7.5. The crystals were cryoprotected by stepwise addition (5% each) of ethylene glycol, up to a final concentration of 25%, and then flash cooled in liquid nitrogen. Diffraction data were collected at 100K on the beamline 12-2 (wavelength: 0.97950 Å) at the Stanford Synchrotron Radiation Lightsource and processed with HKL2000 [40]. Initial phases were determined by molecular replacement using Phaser [41]. Refinement was carried out in Phenix [42], alternating with manual rebuilding and adjustment in COOT [43]. Final refinement statistics are summarized in Table 1. In the final model, 89.3% of the residues were in favored regions of the Ramachandran plot, with 8.9% in additional allowed regions.

Crystallization and structural determination of the 8M2–H2 complex

An excess of purified, recombinant 8M2 Fab was mixed with H2 HA (A/Japan/305+/1957) and incubated overnight at room temperature to allow complex formation. The optimal ratio was pre-determined by titration of Fab to HA as assayed by gel-shift using BN-PAGE. The complex was purified from excess Fab by gel filtration in 20 mM Tris pH 8.0, 100 mM NaCl, and concentrated to 8.8 mg/mL for crystallization. 8M2-H2 complex crystals were grown at 20°C in sitting drops by vapor diffusion against a reservoir containing 10% PEG6000, 0.1 M Na citrate, pH 4 and 1 M LiCl. The crystals were cryoprotected by soaking in a buffer containing 7 µl mother liquor and 3 µl ethylene glycol, and then flash cooled in liquid nitrogen. Diffraction data were collected at 100K on the GM/CA-CAT 23ID-B beamline (wavelength: 1.0332 Å) at the Advanced Photon Source and processed with HKL2000 [40]. Initial phases were determined by molecular replacement using Phaser [41]. Refinement was carried out in Phenix [42], alternating with manual rebuilding and adjustment in COOT [43]. Final refinement statistics are summarized in Table 1. In the final model, 94.1% of the residues were in favored regions of the Ramachandran plot, with 4.8% in additional allowed regions.

HA glycan binding assays

The gene corresponding to the ectodomain of tested hemagglutinin (HA) was expressed as described [39]. Supernatant from the suspension culture of insect Sf9 cells was batch purified using Ni-NTA resin (Qiagen). Fractions containing HA0 were purified through size-exclusion chromatography and concentrate to 1 mg/ml in 20 mM Tris-HCl, 100 mM NaCl,

pH 8.0. Procedures for HA glycan microarray binding assay were described previously [44]. A list of glycans on the microarray is included in Supplementary Table 1.

Supplementary Material

Refer to Web version on PubMed Central for supplementary material.

Acknowledgments

The work was supported in part by NIH grants AI058113 (I.A.W., J.E.C. and J.C.P.) and R01 AI106002 (J.E.C.), DOD grant HDTRA1-08-10-BRCWMD-BAA and NIH contract HHSN272200900047C (J.E.C.), the Skaggs Institute for Chemical Biology, the Scripps Microarray Core Facility, and a contract from the Centers for Disease Control (J.C.P.). Glycans used for HA binding assay were partially provided by the Consortium for Functional Glycomics (http://www.functionalglycomics.org/) funded by NIGMS grant GM62116 (J.C.P.). We thank W. Yu and X. Dai (The Scripps Research Institute) for excellent technical support. This is publication 21487 from The Scripps Research Institute.

X-ray diffraction datasets were collected at the Advanced Photon Source beamline 23ID-B (GM/CA CAT) and the Stanford Synchrotron Radiation Lightsource beamline 12-2. GM/CA CAT has been funded in whole or in part with federal funds from the National Cancer Institute (Y1-CO-1020) and the National Institute of General Medical Sciences (Y1-GM-1104). Use of the Advanced Photon Source was supported by the U.S. Department of Energy, Basic Energy Sciences, Office of Science, under contract No. DE-AC02-06CH11357. The Stanford Synchrotron Radiation Lightsource is a Directorate of SLAC National Accelerator Laboratory and an Office of Science User Facility operated for the U.S. Department of Energy Office of Science by Stanford University. The SSRL Structural Molecular Biology Program is supported by the DOE Office of Biological and Environmental Research, and by the National Institutes of Health, National Institute of General Medical Sciences (including P41GM103393) and the National Center for Research Resources (P41RR001209). The contents of this publication are solely the responsibility of the authors and do not necessarily represent the official views of NIGMS, NCRR or NIH.

References

1. Gilbert SC. Advances in the development of universal influenza vaccines. Influenza Other Respi Viruses. 2012
2. Ekiert DC, Wilson IA. Broadly neutralizing antibodies against influenza virus and prospects for universal therapies. Curr Opin Virol. 2012; 2:134–41. [PubMed: 22482710]
3. Du J, Cross TA, Zhou HX. Recent progress in structure-based anti-influenza drug design. Drug Discov Today. 2012; 17:1111–20. [PubMed: 22704956]
4. Skehel J, Wiley D. Receptor binding and membrane fusion in virus entry: the influenza hemagglutinin. Annu Rev Biochem. 2000; 69:531–69. [PubMed: 10966468]
5. Paulson, JC. The Receptors. Vol. 2. Academic Press; Orlando, FL: 1985. Interactions of animal viruses with cell surface receptors; p. 131-219.
6. Weis W, et al. Structure of the influenza virus haemagglutinin complexed with its receptor, sialic acid. Nature. 1988; 333:426–31. [PubMed: 3374584]
7. Matrosovich M, Klenk HD. Natural and synthetic sialic acid-containing inhibitors of influenza virus receptor binding. Rev Med Virol. 2003; 13:85–97. [PubMed: 12627392]
8. Sauter NK, et al. Hemagglutinins from two influenza virus variants bind to sialic acid derivatives with millimolar dissociation constants: a 500-MHz proton nuclear magnetic resonance study. Biochemistry. 1989; 28:8388–96. [PubMed: 2605190]
9. Vigerust DJ, Shepherd VL. Virus glycosylation: role in virulence and immune interactions. Trends Microbiol. 2007; 15:211–8. [PubMed: 17398101]
10. Sagar M, Wu X, Lee S, Overbaugh J. Human immunodeficiency virus type 1 V1–V2 envelope loop sequences expand and add glycosylation sites over the course of infection, and these modifications affect antibody neutralization sensitivity. J Virol. 2006; 80:9586–98. [PubMed: 16973562]
11. Wilson IA, Cox NJ. Structural basis of immune recognition of influenza virus hemagglutinin. Annu Rev Immunol. 1990; 8:737–71. [PubMed: 2188678]

12. Whittle JR, et al. Broadly neutralizing human antibody that recognizes the receptor-binding pocket of influenza virus hemagglutinin. Proc Natl Acad Sci USA. 2011; 108:14216–21. [PubMed: 21825125]
13. Ekiert DC, et al. Cross-neutralization of influenza A viruses mediated by a single antibody loop. Nature. 2012; 489:526–32. [PubMed: 22982990]
14. Lee PS, et al. Heterosubtypic antibody recognition of the influenza virus hemagglutinin receptor binding site enhanced by avidity. Proc Natl Acad Sci USA. 2012; 109:17040–5. [PubMed: 23027945]
15. Ohshima N, et al. Naturally occurring antibodies in humans can neutralize a variety of influenza virus strains, including H3, H1, H2, and H5. J Virol. 2011; 85:11048–57. [PubMed: 21865387]
16. Krause JC, et al. Human monoclonal antibodies to pandemic 1957 H2N2 and pandemic 1968 H3N2 influenza viruses. J Virol. 2012; 86:6334–40. [PubMed: 22457520]
17. Yoshida R, et al. Cross-protective potential of a novel monoclonal antibody directed against antigenic site B of the hemagglutinin of influenza A viruses. PLoS Pathog. 2009; 5:e1000350. [PubMed: 19300497]
18. Serfling RE, Sherman IL, Houseworth WJ. Excess pneumonia-influenza mortality by age and sex in three major influenza A2 epidemics, United States, 1957–58, 1960 and 1963. Am J Epidemiol. 1967; 86:433–41. [PubMed: 6058395]
19. Housworth J, Langmuir AD. Excess mortality from epidemic influenza, 1957-1966. Am J Epidemiol. 1974; 100:40–8. [PubMed: 4858301]
20. Simonsen L, et al. Pandemic versus epidemic influenza mortality: a pattern of changing age distribution. J Infect Dis. 1998; 178:53–60. [PubMed: 9652423]
21. Nabel GJ, Wei CJ, Ledgerwood JE. Vaccinate for the next H2N2 pandemic now. Nature. 2011; 471:157–8. [PubMed: 21390107]
22. Schafer JR, et al. Origin of the pandemic 1957 H2 influenza A virus and the persistence of its possible progenitors in the avian reservoir. Virology. 1993; 194:781–8. [PubMed: 7684877]
23. Ma W, et al. Identification of H2N3 influenza A viruses from swine in the United States. Proc Natl Acad Sci USA. 2007; 104:20949–54. [PubMed: 18093945]
24. Kaverin NV, et al. Cross-protection and reassortment studies with avian H2 influenza viruses. Arch Virol. 2000; 145:1059–66. [PubMed: 10948982]
25. Huang CC, et al. Structural basis of tyrosine sulfation and VH-gene usage in antibodies that recognize the HIV type 1 coreceptor-binding site on gp120. Proc Natl Acad Sci USA. 2004; 101:2706–11. [PubMed: 14981267]
26. Chan CH, Hadlock KG, Foung SK, Levy S. V(H)1-69 gene is preferentially used by hepatitis C virus-associated B cell lymphomas and by normal B cells responding to the E2 viral antigen. Blood. 2001; 97:1023–6. [PubMed: 11159532]
27. Marasca R, et al. Immunoglobulin gene mutations and frequent use of VH1-69 and VH4-34 segments in hepatitis C virus-positive and hepatitis C virus-negative nodal marginal zone B-cell lymphoma. Am J Pathol. 2001; 159:253–61. [PubMed: 11438472]
28. Carbonari M, et al. Hepatitis C virus drives the unconstrained monoclonal expansion of VH1-69-expressing memory B cells in type II cryoglobulinemia: a model of infection-driven lymphomagenesis. J Immunol. 2005; 174:6532–9. [PubMed: 15879157]
29. Zhou T, et al. Structural definition of a conserved neutralization epitope on HIV-1 gp120. Nature. 2007; 445:732–7. [PubMed: 17301785]
30. Luftig MA, et al. Structural basis for HIV-1 neutralization by a gp41 fusion intermediate-directed antibody. Nat Struct Mol Biol. 2006; 13:740–7. [PubMed: 16862157]
31. Ekiert DC, et al. Antibody recognition of a highly conserved influenza virus epitope. Science. 2009; 324:246–51. [PubMed: 19251591]
32. Sui J, et al. Structural and functional bases for broad-spectrum neutralization of avian and human influenza A viruses. Nat Struct Mol Biol. 2009; 16:265–73. [PubMed: 19234466]
33. Krissinel E, Henrick K. Inference of macromolecular assemblies from crystalline state. J Mol Biol. 2007; 372:774–97. [PubMed: 17681537]

34. Xu R, McBride R, Paulson JC, Basler CF, Wilson IA. Structure, receptor binding, and antigenicity of influenza virus hemagglutinins from the 1957 H2N2 pandemic. J Virol. 2010; 84:1715–21. [PubMed: 20007271]

35. Okuno Y, Isegawa Y, Sasao F, Ueda S. A common neutralizing epitope conserved between the hemagglutinins of influenza A virus H1 and H2 strains. J Virol. 1993; 67:2552–8. [PubMed: 7682624]

36. Yamada A, Brown LE, Webster RG. Characterization of H2 influenza virus hemagglutinin with monoclonal antibodies: influence of receptor specificity. Virology. 1984; 138:276–86. [PubMed: 6208682]

37. Krause JC, et al. Epitope-specific human influenza antibody repertoires diversify by B cell intraclonal sequence divergence and interclonal convergence. J Immunol. 2011; 187:3704–11. [PubMed: 21880983]

38. Liu J, et al. Structures of receptor complexes formed by hemagglutinins from the Asian Influenza pandemic of 1957. Proc Natl Acad Sci USA. 2009; 106:17175–80. [PubMed: 19805083]

39. Xu R, et al. Structural basis of preexisting immunity to the 2009 H1N1 pandemic influenza virus. Science. 2010; 328:357–60. [PubMed: 20339031]

40. Otwinowski Z, Minor W. Processing of X-ray diffraction data collected in oscillation mode. Meth Enzymol. 1997; 276:307–326.

41. McCoy AJ, Grosse-Kunstleve RW, Storoni LC, Read RJ. Likelihood-enhanced fast translation functions. Acta Cryst. 2005; D6164:458.

42. Adams PD, et al. PHENIX: building new software for automated crystallographic structure determination. Acta Cryst. 2002; D58:1948–54.

43. Emsley P, Cowtan K. Coot: model-building tools for molecular graphics. Acta Cryst. 2004; D60:2126–32.

44. Xu R, McBride R, Nycholat CM, Paulson JC, Wilson IA. Structural characterization of the hemagglutinin receptor specificity from the 2009 H1N1 influenza pandemic. J Virol. 2012; 86:982–90. [PubMed: 22072785]

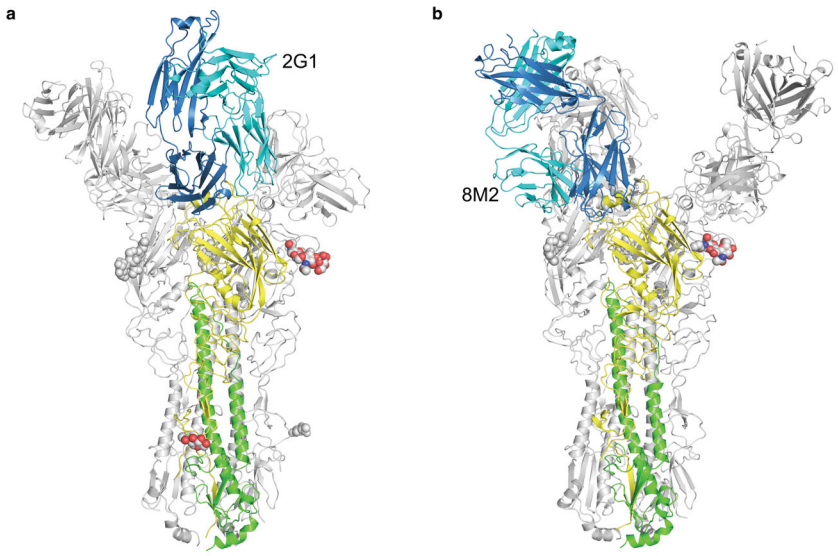

Fig. 1.

Crystal structures of H2 HA in complex with Fab 2G1 (**a**) and Fab 8M2 (**b**). Three Fabs are associated with each HA trimer. One of the Fabs is colored in blue (heavy chain) and cyan (light chain) and the corresponding HA1 in yellow and HA2 in green. N-linked glycans that are observed in the crystal structure are shown in spheres (carbon in grey, oxygen in red and nitrogen in blue). The other two protomers in the HA trimer and their associated Fabs are colored in light grey.

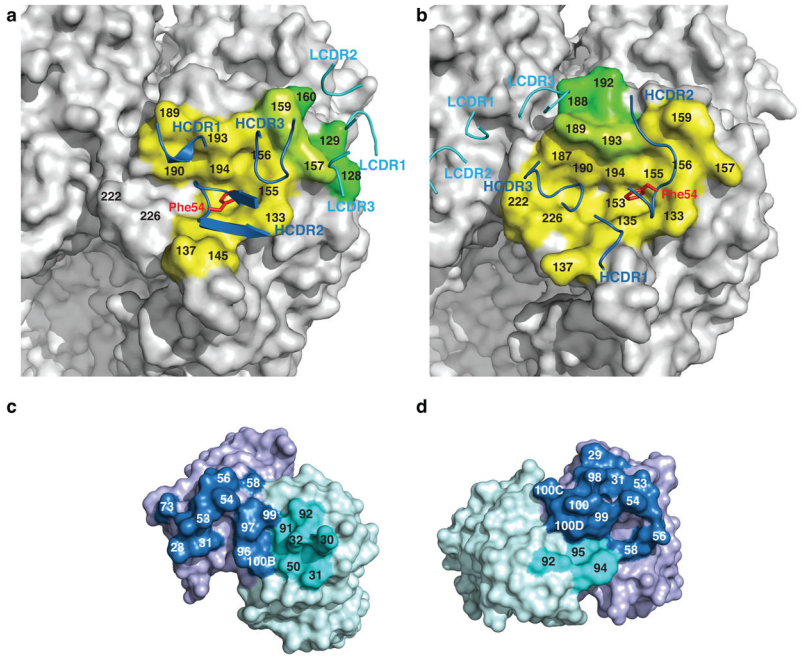

Fig. 2.

Antibody–antigen binding footprints in the 2G1 and 8M2 complexes. (**a**) Footprint of 2G1 on the HA. HA residues interacting with the heavy-chain are colored in yellow with the light chain contacts in green. Residues in contact with both heavy and light chains are shown in light green. CDR loops are shown in ribbons. Phe54 on HCDR2 inserts into the receptor-binding pocket and is highlighted in red sticks. (**b**) Footprint of 8M2 on the HA. HA and CDR loops are colored as in panel A. (**c**) Footprint of HA on 2G1 combining site. (**d**) Footprint of HA on 8M2 combining site. Antibody residues in contact with HA are shown in darker colors (heavy chain in blue on a purple background and light chain in cyan on a whitish cyan background).

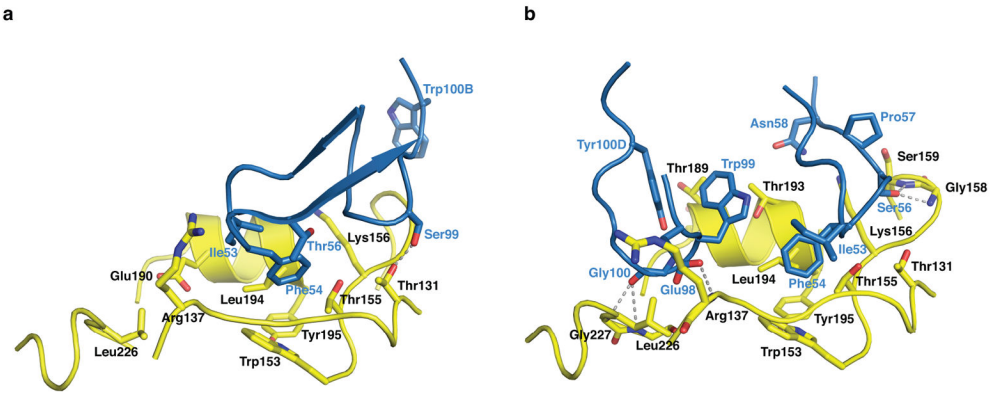

Fig. 3.

Recognition of the receptor-binding site by the HCDR2 and HCDR3 loops of 2G1 (**a**) and 8M2 (**b**). In the crystal structures, antibodies 2G1 and 8M2 approach the HA from completely opposite orientations, with the two HCDR3s interacting on opposite ends of the receptor-binding site, rotated around HCDR2 by approximately 180°. The signature motif of antibodies encoded by germline gene V_H1-69 is the hydrophobic tip of HCDR2 loop containing Ile53 and Phe54. In both structures, Phe54 is buried in the conserved hydrophobic pocket formed by Trp153 and neighboring residues of HA1, where sialic acid binds. The rest of the HCDR2 loop and the HCDR3 residues contact different parts of the HA receptor-binding site. Residues key to the interaction are highlighted in sticks, and hydrogen bonds are shown in dashed lines.

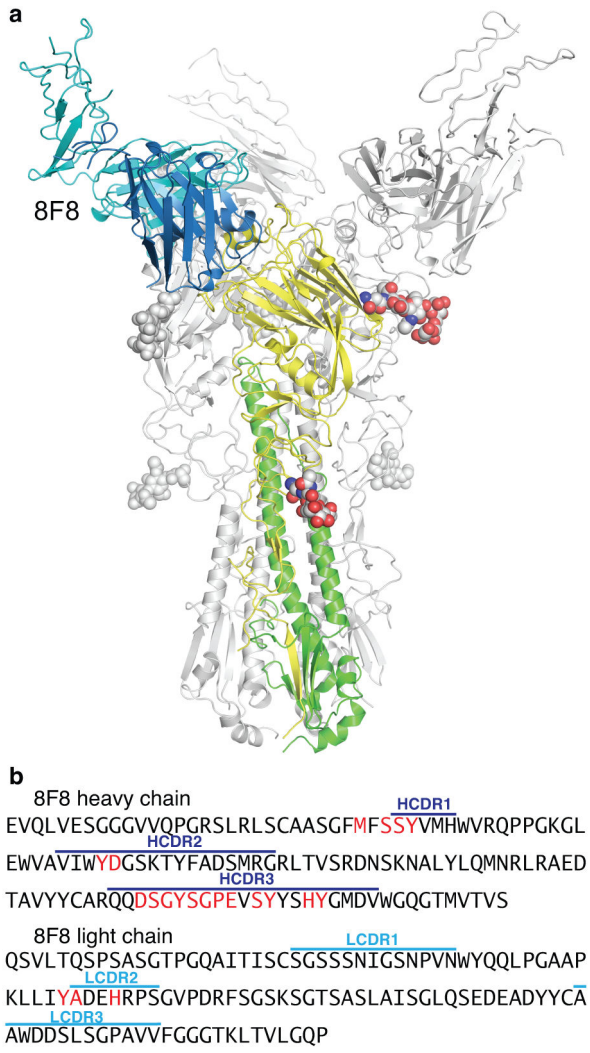

Fig. 4.

Crystal structure of 8F8 with H2 HA. (**a**) Overall structure of the antibody–antigen complex. Three Fabs bind to the HA trimer. Fab 8F8 (heavy chain in blue, light chain in cyan) targets the receptor-binding site of HA (HA1 in yellow and HA2 in green). N-linked glycans that are observed in the crystal structure are shown in spheres (carbon in grey, oxygen in red and nitrogen in blue). The other two protomers in the HA trimer and their associated Fabs are colored in light grey. (**b**) Amino-acid sequences of 8F8 fragment. Residues that are in contact with HA in the complex structure are highlighted in red. 8F8 binding to H2 HA is dominated by the heavy chain.

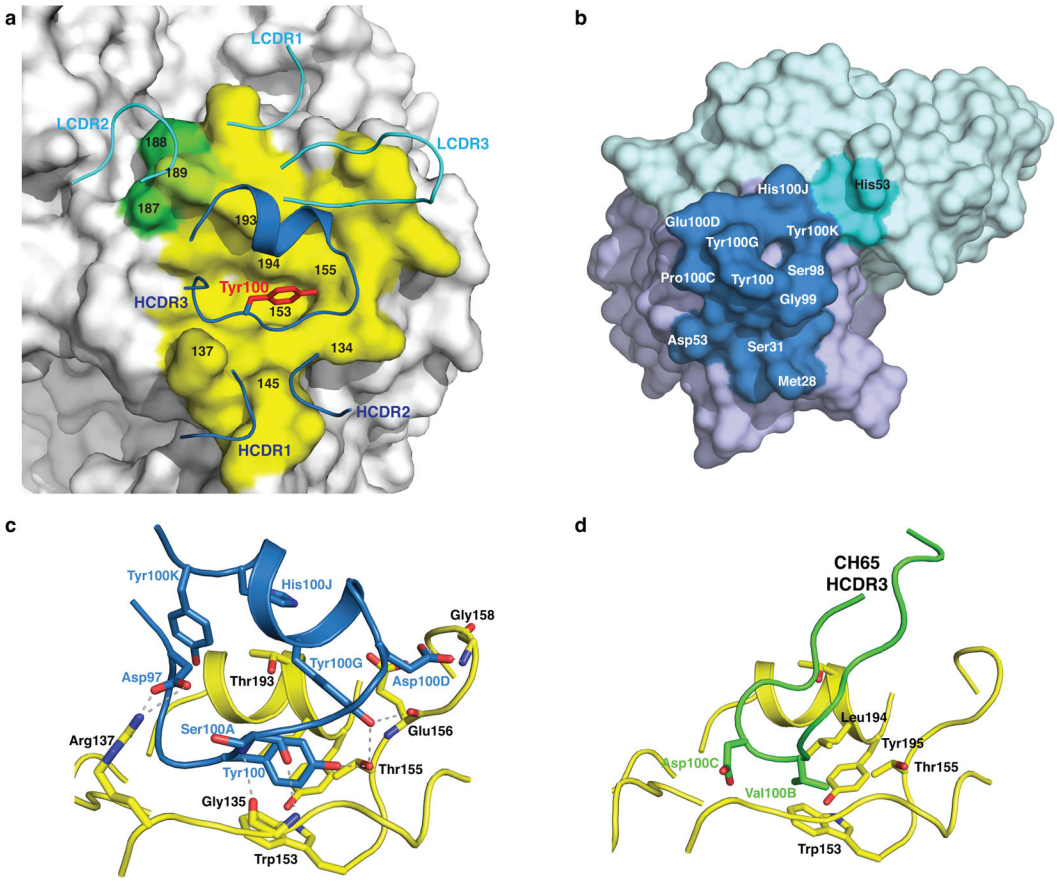

Fig. 5.

Antibody–antigen recognition by 8F8. (**a**) Footprint of 8F8 on the HA. HA residues interacting with the heavy chain are colored in yellow and with the light chain in green. Residues in contact with both heavy and light chains are shown in light green (residue 189). CDR loops are shown in ribbons. Tyr100 (shown as red sticks) on the HCDR3 inserts into a hydrophobic pocket in the receptor-binding site. (**b**) Footprint of HA on 8F8 combining site. Antibody residues in contact with HA are shown in darker colors (heavy chain in blue on a purple background and light chain in cyan on a whitish cyan background). (**c**) At the antibody–antigen interface in the crystal structure, the 8F8 HCDR3 loop dominates the interactions with HA. Residues key to the antibody association are highlighted in sticks and hydrogen bonds are shown in dashed lines. Tyr100forms π-π interactions with HA Trp153. (**d**) Comparison between 8F8 and CH65, an antibody targeting the receptor-binding site of seasonal H1 HA. In the structure of CH65 (ref. [12]), Val100B, instead of Tyr100 in 8F8, occupies the hydrophobic pocket in the receptor-binding site.

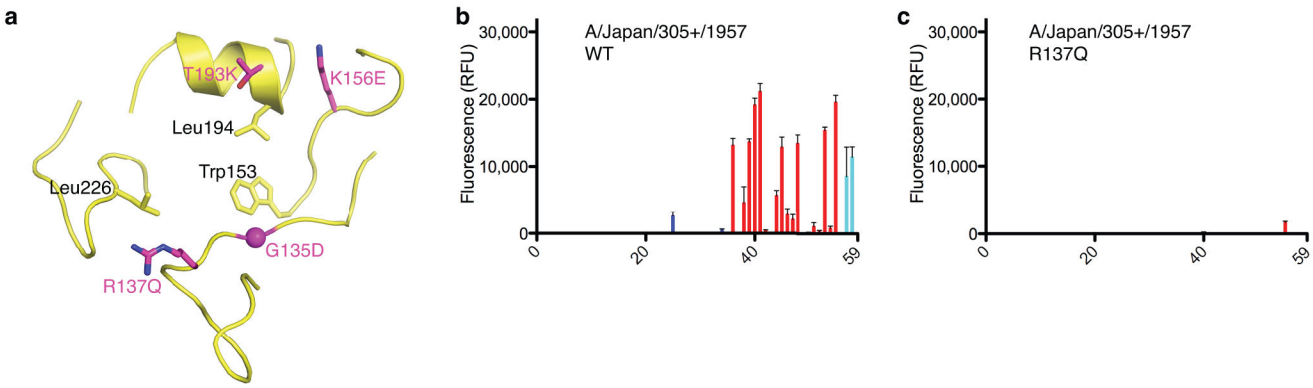

Fig. 6.

Escape mutations on H2 HA for binding to antibodies 8F8, 8M2 and 2G1 and their effects on binding of glycan receptors. (**a**) Escape mutants were identified *in vitro*: R137Q or T193K for 8F8, G135D for 8M2 and K156E for 2G1. (**b**) Glycan binding analysis of recombinant wild-type (WT) H2 HA on glycan microarray. WT H2 HA shows specific binding toward certain α2–6-linked sialylated glycans (red bars; 36 to 56) and glycans of α2–6 and α2–3 mixed linkages (cyan; 57 and 58), but not to α2–3-linked glycans (blue; 3 to 35) or neutral glycans (black; 1 and 2). The list of glycans on the array is provided in Supplementary Table 1. (**c**) The single mutation R137Q abolishes glycan binding (or weakens glycan binding to below the detection threshold) for H2 HA, compared with the WT HA tested under the same conditions. All error bars in the figure are indicative of standard deviation from quadruplicates. Similar results for mutations T193K, G135D or K156E are included in Supplementary Fig. 2.

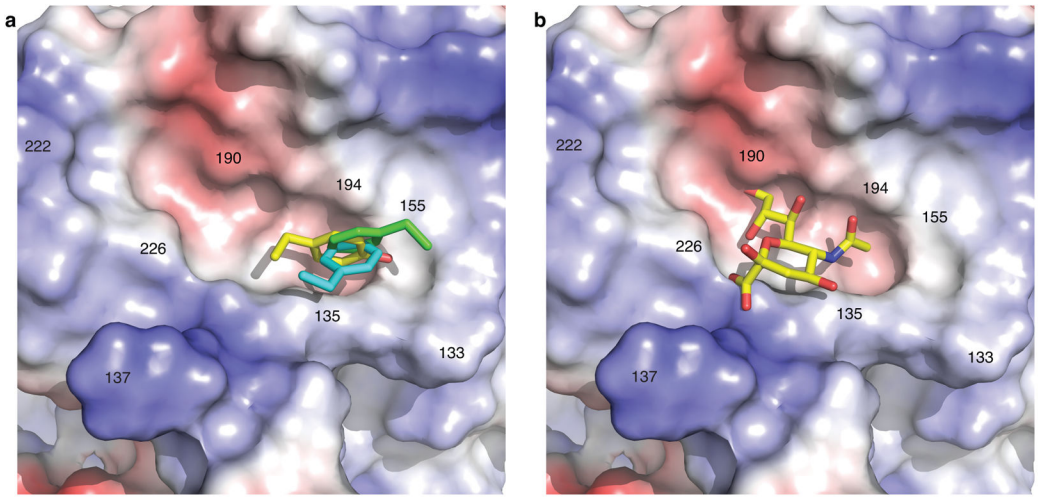

Fig. 7.

Targeting the receptor-binding site. (**a**) Conservation of a key interaction for three H2 antibodies targeting the receptor-binding site of HA. Aromatic residues at the tip of CDR loops (Tyr100 of 8F8 in yellow, Phe54 of 8M2 in green, Phe54 of 2G1 in cyan) insert into the highly conserved hydrophobic pocket of HA in the same pocket that sialic acid of the glycan receptor binds (HA is shown in electrostatic surface representation (positive charges in blue, negative charges in red and neutral in white). (**b**) The location for binding of sialic acid in the receptor-binding site was modeled based on the crystal structure of H2 HA in complex with human receptor analog LS-Tetrasaccharide c (LSTc) (PDB code: 2WRE [38]).

Table 1

Data collection and refinement statistics (molecular replacement)

	8F8-H2	8M2-H2	2G1-H2
Data collection			
Space group	P321	H32	$P2_12_12_1$
Cell dimensions			
a, *b*, *c* (Å)	136.6, 136.6, 142.1	129.6, 129.6, 536.9	126.8, 133.1, 813.0
α, *β*, *γ* (°)	90, 90, 120	90, 90, 120	90, 90, 90
Resolution (Å)	50-3.0 (3.11-3.00) [a]	45-3.1 (3.21-3.10)	50-3.15 (3.26-3.15)
R_{merge}	0.10 (0.59)	0.12 (0.31)	0.13 (0.82)
$I/\sigma I$	11.6 (1.2)	14 (3.6)	11.5 (1.6)
Completeness (%)	94.7 (64.8)	94.6 (63.0)	98.7 (95.6)
Redundancy	3.9 (3.2)	9.2 (5.9)	6.6 (5.5)
Refinement			
Resolution (Å)	44.7-3.0	41.9-3.1	48.1-3.2
No. reflections	27,264	27,299	205,778
R_{work}/R_{free}	22.9%/28.2%	19.3%/25.1%	24.9%/30.2%
No. atoms			
Protein	6,561	7,214	58,356
Ligand/ion	78	28	386
Water	0	0	0
B-factors			
Protein	97.9	63.0	73.5
Ligand/ion	123.4	88.9	103.8
R.m.s. deviations			
Bond lengths (Å)	0.008	0.003	0.010
Bond angles (°)	1.23	0.75	1.37

[a] Values in parentheses are for highest-resolution shell.

[b] One crystal for each structure was used for data collection and structure determination.